Enrichment of lignin-derived carbon in mineral-associated soil organic matter

Wenjuan Huang,[†,∞] *Kenneth E. Hammel,*[‡,§] *Jialong Hao,*[⊥] *Aaron Thompson,*[⊤] *Vitaliy I. Timokhin*[┼] *and Steven J. Hall*[†*].

[†]Department of Ecology, Evolution, and Organismal Biology, Iowa State University, Ames, Iowa 50011, United States

[‡]US Forest Products Laboratory, Madison, WI 53726, United States

[§]Department of Bacteriology, University of Wisconsin, Madison, WI 53706, United States

[⊥]Key Laboratory of Earth and Planetary Physics, Institute of Geology and Geophysics, Chinese Academy of Sciences, Beijing 100029, China

[⊤]Department of Crop and Soil Sciences, The University of Georgia, Athens, Georgia 30602, United States

[┼]University of Wisconsin, Wisconsin Energy Institute, DOE Great Lakes Bioenergy Research Center, Madison, Wisconsin 53706, United States

[∞]Key laboratory of Vegetation Restoration and Management of Degraded Ecosystems, South China Botanical Garden, Chinese Academy of Sciences, Guangzhou 510650, China

ABSTRACT

A modern paradigm of soil organic matter proposes that persistent carbon (C) derives primarily from microbial residues interacting with minerals, challenging older ideas that lignin moieties contribute to soil C because of inherent recalcitrance. We proposed that aspects of these old and new paradigms can be partially reconciled by considering interactions between lignin decomposition products and redox-sensitive iron (Fe) minerals. An Fe-rich tropical soil (with C_4 litter and either ^{13}C-labeled or unlabeled lignin) was pre-treated with different durations of anaerobiosis (0–12 days) and incubated aerobically for 317 days. Only 5.7±0.2% of lignin ^{13}C was mineralized to CO_2 versus 51.2±0.4% of litter C. More added lignin-derived C (48.2±0.9%) than bulk litter-derived C (30.6±0.7%) was retained in mineral-associated organic matter (MAOM; density > 1.8 g cm^{-3}), and 12.2±0.3% of lignin-derived C vs. 6.4± 0.1% of litter C accrued in clay-sized (< 2 μm) MAOM. Longer anaerobic pre-treatments increased added lignin-derived C associated with Fe, according to extractions and nanoscale secondary ion mass spectrometry (NanoSIMS). Microbial residues are important, but lignin-derived C may also contribute disproportionately to MAOM relative to bulk litter-derived C—especially following redox-sensitive biogeochemical interactions.

TOC Art

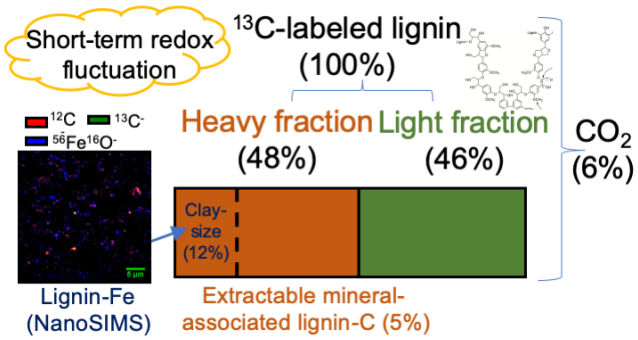

INTRODUCTION

Lignin is critically linked to our understanding of terrestrial carbon (C) cycling given its importance in controlling initial rates of litter decomposition, and its high overall C loading to the environment—lignin is the second most abundant plant-derived organic substance after cellulose.[1,2] Lignin was historically thought to contribute disproportionately to soil organic matter (SOM) relative to other organic compounds as a consequence of its complex macromolecular structure,[3] which requires strong, non-specific oxidants for depolymerization.[4] However, a modern paradigm of SOM dynamics[5,6] proposes that environmental, biological, and geochemical controls, rather than molecular structure alone, determine the persistence of SOM. The Microbial Efficiency-Matrix Stabilization (MEMS) hypothesis proposes that C derived from labile constituents of plant biomass (e.g., unprotected cellulose) which are efficiently converted to microbial biomass and necromass (i.e., compounds with high C-use efficiency) tend to accrue in SOM by interacting with mineral surfaces and facilitating aggregate formation.[5,7–10] In contrast, C from complex polymers such as lignin tends to have poor microbial C-use efficiency (as low as 1%[11,12] to 8 – 31%[13]) and is more likely to be lost as CO_2 than to contribute to mineral-associated organic matter (MAOM).[8] However, this framework does not fully consider

60 the impacts of compound-specific interactions between SOM constituents and minerals, which
61 may be especially important in soils with large proportions of reactive secondary minerals.[14]

62 Fe (oxyhydr)oxides and short-range-ordered (SRO) Fe phases in particular are widely
63 understood to protect SOM from microbial decomposition via sorption and co-precipitation, and
64 these phases may preferentially associate with aromatic lignin decomposition products relative to
65 other organic compounds.[15–19] Soils undergoing short-term redox fluctuations can generate
66 significant amounts of SRO Fe phases,[20–22] which would potentially increase the capacity for
67 adsorbing or co-precipitating lignin-derived C. Although lignin decomposition can be sustained
68 under fluctuating redox environments,[23] sorption of lignin decomposition products to freshly-
69 formed SRO phases[17,18] may provide a mechanism for incorporation of lignin-derived C in
70 MAOM. Lignin decomposition products can potentially contribute significantly to MAOM,[15,16]
71 yet the fates of lignin during decomposition in soil remain poorly understood. Here, we propose
72 that lignin represents a more important contributor to MAOM than recently acknowledged due to
73 interactions with Fe mineral phases, and that these interactions vary significantly as a function of
74 soil redox conditions.

75 Analytical challenges have presented major barriers in resolving ongoing controversies
76 about lignin decomposition in soil. The common assays of lignin residues using cupric oxide
77 oxidation can potentially obscure the importance of lignin in MAOM due to failure to recover
78 significant amounts of lignin sorbed on soil minerals.[24,25] Nuclear magnetic resonance analyses
79 of SOM frequently require removal of Fe by strong acid pre-treatment, causing potentially
80 significant loss and possible chemical fractionation of SOM.[26] Solution-phase analyses of SOM
81 such as ultrahigh resolution spectroscopy (FT-ICR-MS) can be very powerful,[15] but quantitative
82 solubilization of SOM is difficult.[5] The addition of isotope-labeled synthetic lignins to soil can

surmount these challenges by allowing unambiguous measurements of lignin mineralization to CO_2 and incorporation of lignin-derived C in microbial biomass.[11,12,27] The potential flux of lignin-derived C through microbial biomass can also be constrained using measurements of lignin mineralization and estimates of microbial C-use efficiency, and residual lignin-derived C in the solid phase can be quantified by combustion of solid organic matter to CO_2. However, isotope-labeled synthetic lignins have not been widely used in soils since the seminal work of Haider and colleagues.[11,12,27]

Here, we tested the hypotheses that 1) added lignin-derived C contributes disproportionately to MAOM relative to C derived from bulk litter, due to differential sorption or co-precipitation with Fe, and 2) a short-term redox fluctuation has lasting impacts on the fate of added lignin-derived C. We collected soil from a tropical forest (C_3 vegetation) rich in reactive Fe minerals that experiences frequent O_2 fluctuations driven by episodic rainfall and high rates of microbial metabolism.[28,29] The soil was amended with leaf litter from a C_4 grass and either synthetic ^{13}C-labeled or unlabeled lignin, which enabled us to discriminate between three different C sources (soil-C, bulk litter-C, and lignin-C labeled at C_β of the propyl sidechain). Release of lignin $^{13}C_\beta$ as CO_2 demonstrates unequivocally that the polymer was cleaved.[4] Soil samples were pre-treated with either 12, 8, 4, and 0 days of anaerobiosis to generate a gradient of redox conditions representative of field conditions,[29] and subsequently exposed to an aerobic headspace for 317 days.

MATERIALS AND METHODS

Sample Preparation. Soil (A horizon, 0 – 10 cm) was collected from an upland valley in a perhumid tropical forest near the El Verde field station of the Luquillo Experimental Forest (18°17′N, 65°47′W), Puerto Rico. Leaves and fine roots of the dominant tree species at this site contain significant lignin (12 – 29% by mass[30]), as is typical for most higher plants.[1] This soil experiences temporal O_2 fluctuations in surface horizons, which in turn stimulate Fe redox cycling,[29] and is an Oxisol developed from basaltic to andesitic volcaniclastic sediments.[21] The sample was shipped overnight to Iowa State University and passed through an 8-mm sieve to remove coarse roots while retaining micro-aggregate structure (rocks are absent in the < 8-mm fraction of this soil). Soil was gently mixed and brought to field moisture capacity (1.0 g H_2O g^{-1} soil). Subsamples (1 g dry mass equivalent) were incubated according to three substrate treatments to partition respiration from soil, litter (senesced leaves of *Andropogon gerardii*; see the Supporting Information (SI) for further details), and the C_β position of the added ^{13}C-labeled lignin: (1) soils alone (control); (2) soils amended with litter and synthetic lignin (soil + litter + unlabeled lignin) and (3) soils amended with litter and synthetic lignin labeled with 99 atom% ^{13}C at the C_β position of each lignin C_9 substructure (soil + litter + $^{13}C_\beta$-labeled lignin). The synthetic lignin had been fractionated prior to the experiment by gel permeation chromatography to obtain polymeric lignins with a molecular mass greater than 1 kDa. Similar to natural lignin, macromolecular synthetic lignin is insoluble in water until it is depolymerized to lower-molecular-weight constituents during decomposition.[31] Each subunit had an average molecular mass of 197, such that the ^{13}C label represented 13/197 of the added synthetic lignin mass. The lyophilized unlabeled or labeled lignins were precipitated in a 1:21 mass ratio on dried and finely ground leaf litter of *Andropogon gerardii* (big bluestem, a C_4 grass), which provided an isotopic contrast with C_3-derived soil C (see SI for more details). Leaf litter of *Andropogon gerardii* (no

127 stem) was collected shortly after senescence, and had 41.3% C and 1.1% N. Soils were gently
128 homogenized with the litter + lignin mixtures in a 9:1 ratio (0.9 g dry soil mass mixed with 99
129 mg litter and 4.74 mg lignin for each soil sample). The ratio of added C (litter + lignin mixtures)
130 to SOC was ~42:31 for each sample. In this paper, "lignin-derived C" hereafter refers to the $^{13}C_{\beta}$
131 moiety of the synthetic lignin added to the litter; the *A. gerardii* litter also contained natural
132 lignin.

133 **Headspace Treatments.** Soil samples were incubated in the dark for 329 days in total at
134 laboratory temperature (23 ± 1 °C) in glass jars (946 mL) sealed with Viton gaskets and
135 aluminum lids with butyl septa. Over the first 12 days of the experiment, samples were exposed
136 to CO_2-free air and/or dinitrogen (N_2) headspaces to impose varying durations of anaerobiosis at
137 staggered intervals (12, 8, 4, and 0 days). We refer to the first 12 days as the "anaerobic pre-
138 treatment" phase of the experiment, which mimics the short-term deprivation of oxygen that soils
139 frequently experience in this ecosystem.[28,29] Specifically, during the pre-treatment, samples were
140 exposed to aerobic conditions for 12 days (0-day anaerobic pre-treatment, control), for 8 days
141 followed by a 4-day anaerobic phase (4-day anaerobic pre-treatment), for 4 days followed by an
142 8-day anaerobic phase (8-day anaerobic pre-treatment) and for 0 days (12-day anaerobic pre-
143 treatment). After day 12 all samples were exposed to an aerobic headspace for the subsequent
144 317 days. Anaerobic conditions were attained by flushing jars with ultrapure N_2, and aerobic
145 conditions were attained using CO_2-free air. Jars were re-flushed with the appropriate gas
146 following periodic headspace sampling as described below. Soil moisture was monitored by
147 recording the mass of each sample, and water was added as necessary throughout the experiment
148 to replace moisture lost during headspace flushing. Blank jars (without soil) were similarly
149 treated as the samples.

Partitioning of CO_2 Sources. Headspace gas was initially measured every two days for soils with litter + lignin and every four days for control soils (to ensure sufficient accumulation of CO_2 for precise analyses in the latter treatment).[32] After 47 days, samples were measured weekly, and after 189 days, every two weeks. We measured CO_2 concentrations and their $\delta^{13}C$ values immediately prior to flushing the headspace. Gas was sampled via a 5-mL syringe with stopcock and immediately injected into a carrier gas (CO_2-free air) flowing into a tunable diode laser absorption spectrometer (TDLAS, TGA200A, Campbell Scientific, Logan, UT). Concentrations of CO_2 and $\delta^{13}C$ values were calibrated following Hall et al.[32] The production of CO_2 derived from soil, litter and $^{13}C_\beta$-labeled lignin was calculated by mixing models[32] described in the SI. Additional headspace gas samples (20 mL) were collected for CH_4 measurements during the first 105 days, after which CH_4 production was negligible. Concentrations of CH_4 were analyzed by gas chromatography with a flame ionization detector (GC-2014, Shimadzu, Columbia, MD). However, impacts of CH_4 production on ^{13}C mass balance were negligible in this experiment as CH_4 accounted for <1% of total C mineralization.[33] The CO_2 production from soil, litter and lignin was expressed relative to dry mass of the whole sample (soil + litter + lignin). All other element fluxes or concentrations were expressed similarly.

Carbon in Different Soil Fractions. At the end of this experiment, a combined density and particle size fractionation was conducted to remove free light organic matter and separate high-density fractions (> 1.8 g cm^{-3}) and the clay-sized subset of the high-density fractions (< 2 μm) in the samples with litter and unlabeled/$^{13}C_\beta$-labeled lignin (n = 24) to quantify the lignin-and litter-derived C in different soil fractions (see SI for more details). Briefly, sodium polytungstate solution (density 1.8 g cm^{-3})[34] was used to remove light fractions from heavy fractions. Samples were shaken overnight to gently disperse aggregates rather than applying sonication, which can

cause organo-mineral associations to be released in lighter fractions.[35] The clay-sized fractions were then separated from remainder of the heavy fractions by centrifugation and masses of each were recorded. The C concentrations and $\delta^{13}C$ values of both the clay-sized and non-clay-sized portions of the heavy fractions in the $^{13}C_{\beta}$-labeled lignin samples were analyzed at the UC Davis Stable Isotope Facility using an elemental analyzer (Elementar Analysensysteme GmbH, Hanau, Germany) and continuous flow isotope ratio mass spectrometer (Sercon Ltd., Cheshire, UK), and unlabeled samples were similarly analyzed at Iowa State University (ThermoFinnigan Delta Plus XL, Waltham, MA). We used previous data to estimate $\delta^{13}C$ values of the initial dense fraction SOM (-27.6‰) in the mixing model.[36]

Selective Extractions. Subsamples of bulk (non-density-fractionated) soil were extracted by sodium dithionite ($Na_2S_2O_4$, used to reductively dissolve Fe phases) and subsequent sodium pyrophosphate ($Na_4P_2O_7$, used to complex Fe and Al) [37,38] to examine anaerobic pre-treatment effects on Fe (oxyhydr)oxides and associated organic C at the end of incubation, which was partitioned among soil, litter and lignin using $\delta^{13}C$ values of DOC released in the extraction (see SI for more details).

^{57}Fe Mössbauer Spectroscopy. Iron phases were characterized at the end of the experiment in a subsample of bulk (non-density-fractionated) soil from one replicate from each headspace treatment by ^{57}Fe Mössbauer spectroscopy. This method has been previously used to investigate soil Fe abundance and composition and their relationships with SOM.[20,21,36,39] We recorded spectra at 140, 77, and 5K to evaluate the crystallinity continuum of Fe^{III} (oxyhydr)oxide phases. We calculated a relative crystallinity index for each sample using the ratio of sextet areas measured at 77K and 5K.[36,39] More information on the ^{57}Fe Mössbauer spectroscopy can be found in SI.

196 **NanoSIMS Analysis.** Finally, to assess spatial relationships among mineral and organic phases,
197 the high-density clay-sized fractions of samples (< 2 μm) that received litter and $^{13}C_{\beta}$-labeled
198 lignin (n = 12) were analyzed by NanoSIMS (Cameca NanoSIMS 50L, Gennevilliers, France) at
199 the Institute of Geology and Geophysics, Chinese Academy of Sciences, Beijing, China (see SI
200 for a detailed description). We used the < 2 μm dense fraction for NanoSIMS for two reasons.
201 First, larger particles decrease the uniformity of the sample surface on the silicon analysis wafer
202 (see SI) and can decrease the resolution of the method. Second, we sought to be conservative in
203 our analysis of organo-mineral associations, acknowledging the potential for incomplete
204 dispersion of microaggregates during density fractionation. Therefore, our NanoSIMS data do
205 not necessarily represent the dense fraction as a whole. NanoSIMS images were analyzed using
206 ImageJ (1.52d version) with the Open MIMS Image plugin.[40] In the NanoSIMS images, the
207 presence of $^{12}C^-$, $^{13}C^-$, and $^{56}Fe^{16}O^-$ ion masses indicated the presence of organic C and Fe
208 minerals, respectively. Based on the $^{56}Fe^{16}O^-$ images, the regions of interest (ROIs) were selected
209 using the threshold option of the ImageJ software with the Otsu method.[41] The same ROIs were
210 simultaneously selected from the other elemental images. We extracted areas and means of
211 secondary ion masses for each ROI from all images. Areas greater than 10 pixels in the ROIs
212 were used for further calculations.

213 **Data Analysis.** Differences in CO_2 production from soils, litter, and lignin among the anaerobic
214 pre-treatments were examined using mixed-effects models, which included treatments as fixed
215 effects and samples as a random effect (to account for temporal correlation within sampling
216 units) using the lmer function in R.[42] Effects of anaerobic pre-treatments on cumulative CO_2
217 production and soil chemical properties were tested by ANOVA, with Duncan tests to compare
218 significant differences among treatments. Relationships between soil chemical properties at the

219 end of the experiment and the duration of anaerobic pre-treatments were also analyzed by linear
220 regression models using the lm function in R. Mean values followed by standard errors were
221 reported. All statistical analyses were conducted with R.[43]

222

223 **RESULTS**

224 **Mineralization of Different C Sources.** Longer anaerobic periods depressed CO_2 production (C
225 mineralization) from soil, litter and especially lignin over the first 12 days (Figure 1); however,
226 mineralization of lignin C increased to a greater extent than did mineralization of soil or litter C
227 following the reintroduction of O_2 (day 12 of this experiment). During 12 to 22 days, longer
228 anaerobic pre-treatments resulted in a pulse of greater C mineralization from soil, litter and
229 lignin after the reintroduction of O_2. Notably, after 119 days, C mineralization from lignin (but
230 not soil or litter) increased once again and diverged markedly among the anaerobic pre-
231 treatments (12-day > control and 4-day, $P < 0.01$; 8-day > 4-day, $P < 0.05$). At the end of the
232 incubation (329 days), the 12-day anaerobic pre-treatment had the highest cumulative lignin C
233 mineralization (20.48 ± 0.98 μg C g^{-1}), followed by the 8-day anaerobic pre-treatment (18.32 ±
234 0.88 μg C g^{-1}), control (17.03 ± 1.31 μg C g^{-1}) and 4-day anaerobic pre-treatment (15.19 ± 0.82
235 μg C g^{-1}) (Figure 1f). The value in the 12-day anaerobic pre-treatments significantly differed
236 from the control ($P = 0.05$) and 4-day anaerobic pre-treatments ($P < 0.01$). The C mineralization
237 from soil and litter was similar among the treatments (7.36 ± 0.14 mg C g^{-1} and 21.15 ± 0.15 mg
238 C g^{-1} on average, respectively).

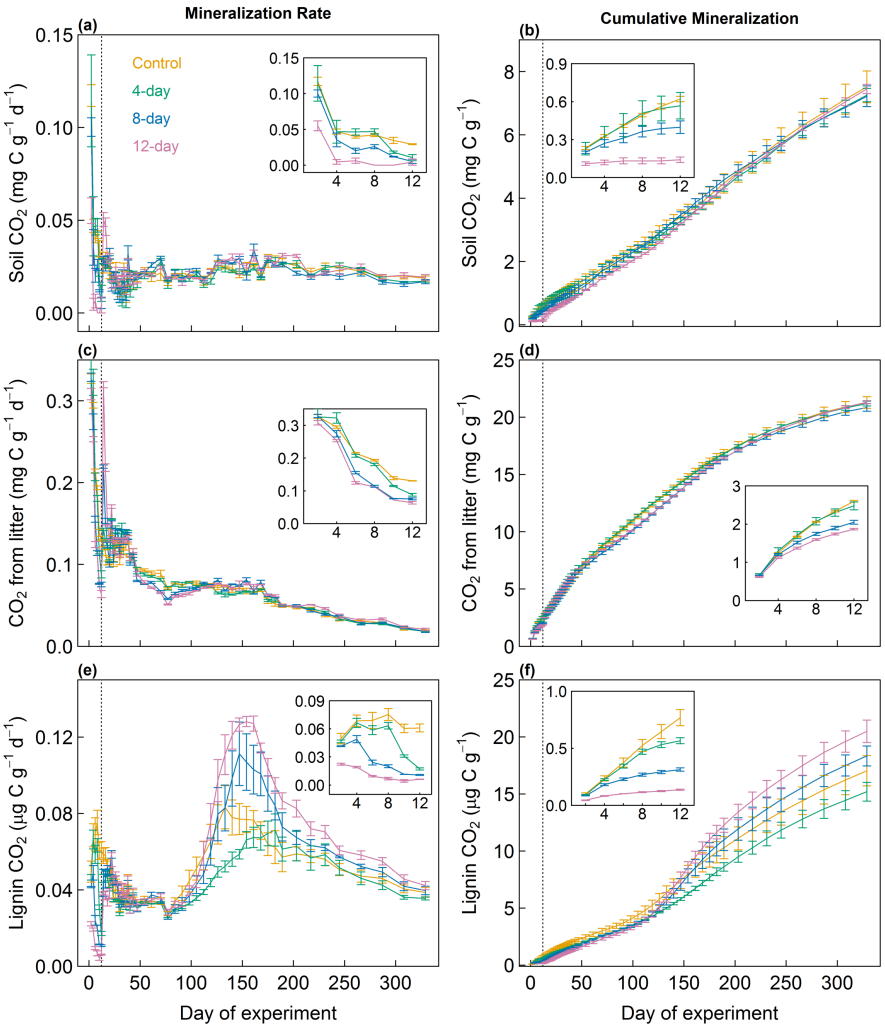

239

240 **Figure 1.** Carbon mineralization (CO_2 production) from soil (a, b), litter (c, d) and synthetic
241 lignin (e, f) in whole soil, expressed relative to dry mass of the whole sample. Insets are
242 expanded views of CO_2 production over the first 12 days. The dotted lines denote the end of
243 anaerobic phase of the pre-treatments at 12 days. The error bars indicate SE (n = 3 for each
244 treatment). Control: continuous aerobic phase during the pre-treatment; 4-day: 8-day aerobic
245 phase followed by 4-day anaerobic phase during the pre-treatment; 8-day: 4-day aerobic phase
246 followed by 8-day anaerobic phase during the pre-treatment; 12-day: 12-day anaerobic phase
247 during the pre-treatment.

Fates of Added Lignin and Litter C. We found that a greater proportion of synthetic lignin-derived C contributed to MAOM than did litter-derived C, across all incubation treatments. Mean C mineralization from lignin accounted for only 5.7 ± 0.2% of initial added lignin ^{13}C, whereas that from litter was 51.2 ± 0.4% of total added litter C (Figure 2). The high-density fractions and their clay-sized subsets (< 2 μm) contained significantly higher proportions of the added lignin-derived C (48.2 ± 0.9% and 12.2 ± 0.3%, respectively) than of litter-derived C (30.6 ± 0.7% and 6.4 ± 0.1%, respectively, $P < 0.01$; Figure 2). The anaerobic pre-treatments did not significantly affect the masses of soil in the high-density fractions, or their corresponding total lignin- or litter-derived C stocks. However, we found a trend of greater clay-sized fraction lignin-derived C in the 4-day (42.5 ± 1.6 μg C g^{-1}) than the 12-day (36.9 ± 2.6 μg C g^{-1}; $P = 0.08$) anaerobic pre-treatment, which was the opposite of that observed for cumulative lignin C mineralization.

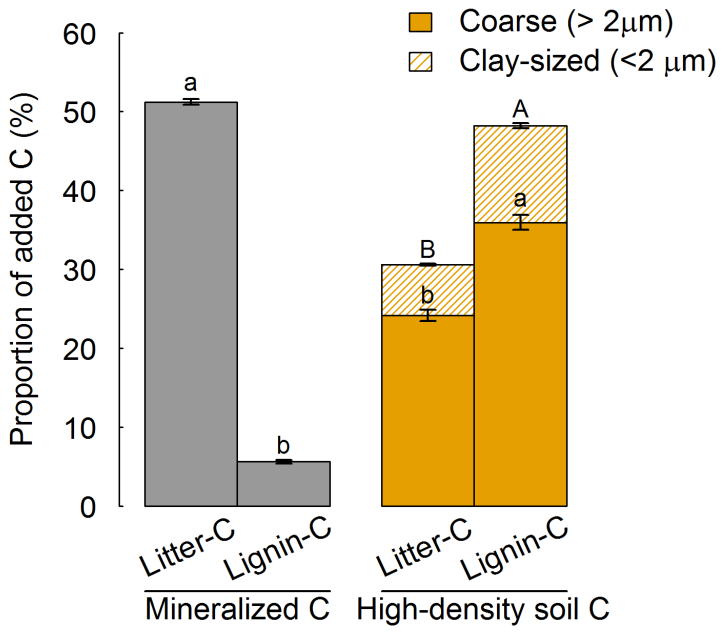

Figure 2. Fates of added lignin and litter C after 329 days. The coarse (> 2 μm) and fine (< 2 μm) portions of the high-density fractions are indicated by solid and hatched bars, respectively. The error bars indicate SE (n = 12). Different lowercase letters indicate significant differences between the litter-C and lignin-C at $P < 0.05$. Different uppercase letters indicate significant differences between the litter-C and lignin-C in the fine portion of the high-density fractions at $P < 0.05$.

Lignin-derived C Associated with Fe Minerals. The mean proportions of added lignin-derived C extracted by dithionite and subsequent pyrophosphate were 1.37 ± 0.06% and 3.31 ± 0.11%, respectively. Increasing the duration of anaerobiosis from 0 to 12 days during the pre-treatment phase yielded significantly more lignin-derived C associated with Fe minerals (and co-occurring Al) at the end of incubation (Figure 3), with no change in litter-derived or soil C. Specifically, lignin-derived C extracted by dithionite and subsequent pyrophosphate significantly increased with the duration of anaerobiosis (3.65 ± 0.22 μg C g^{-1} and 9.18 ± 0.59 μg C g^{-1} in the control vs. 4.91 ± 0.34 μg C g^{-1} and 10.98 ± 0.58 μg C g^{-1} in the 12-day anaerobic pre-treatment, $P < 0.01$ and $P < 0.05$, respectively; Figure 3). In contrast to lignin, soil and litter-derived C extracted by dithionite (4.17 ± 0.06 mg C g^{-1} and 2.03 ± 0.06 mg C g^{-1}, respectively) and subsequent pyrophosphate (7.99 ± 0.09 mg C g^{-1} and 2.31 ± 0.08 mg C g^{-1}, respectively) were similar among treatments.

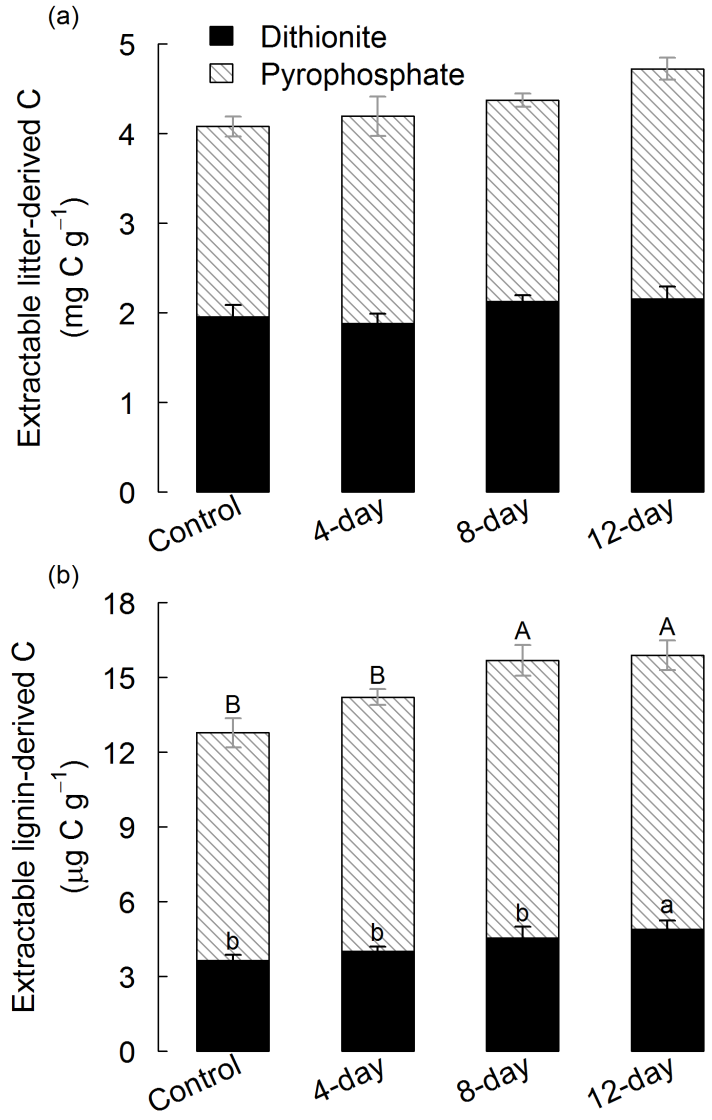

281

282 **Figure 3.** Litter-derived C (a) and lignin-derived C (b) in dithionite and subsequent
283 pyrophosphate extractions of whole soil after 329 days. The error bars indicate SE (n = 3 for
284 each treatment). Different lowercase and uppercase letters indicate significant differences among
285 the treatments at $P < 0.05$ for the dithionite and pyrophosphate extractions, respectively. Control:
286 continuous aerobic phase during the pre-treatment; 4-day: 8-day aerobic phase followed by 4-day
287 anaerobic phase during the pre-treatment; 8-day: 4-day aerobic phase followed by 8-day

288 anaerobic phase during the pre-treatment; 12-day: 12-day anaerobic phase during the pre-
289 treatment.

290

291 No significant differences in concentrations of Fe (oxyhydr)oxides or Fe phase
292 composition were observed among treatments at the end of the experiment, according to the
293 dithionite and secondary pyrophosphate extractions (61.95 ± 0.80 mg Fe g^{-1} and 2.44 ± 0.16 mg
294 Fe g^{-1}, respectively) and ^{57}Fe Mössbauer spectroscopy (Table S1 – 4 and Figure S3 – 6). The
295 dominant Fe phase in soil was nano-goethite, comprising 82.6 ± 0.2% of total Fe, while a
296 ferrihydrite-like phase accounted for 10.5 ± 0.3%. The Fe in primary silicate minerals, silicate
297 clays, and/or surface complexes could not be distinguished by Mössbauer. The Fe(III) and Fe(II)
298 in these phases represented <7% and <0.5% of total Fe, respectively (Supporting information
299 Table S1 – 4 and Figure S3 – 6).

300 NanoSIMS measurements showed that the 8- and 12-day anaerobic pre-treatments
301 increased the amount of lignin-derived C associated with Fe minerals in the high-density clay-
302 sized fractions at the end of the incubation (Figures 4 and S7), despite the similarities in bulk Fe
303 phase compositions among treatments. The regions of interest (ROIs) selected using the $^{56}Fe^{16}O^-$
304 images showed that the 12- and 8-day anaerobic pre-treatments had higher ratios of ($^{12}C^- + {}^{13}C^-$
305)/$^{56}Fe^{16}O^-$ and more ^{13}C associated with Fe minerals than the other treatments ($P < 0.01$; Figure
306 S7).

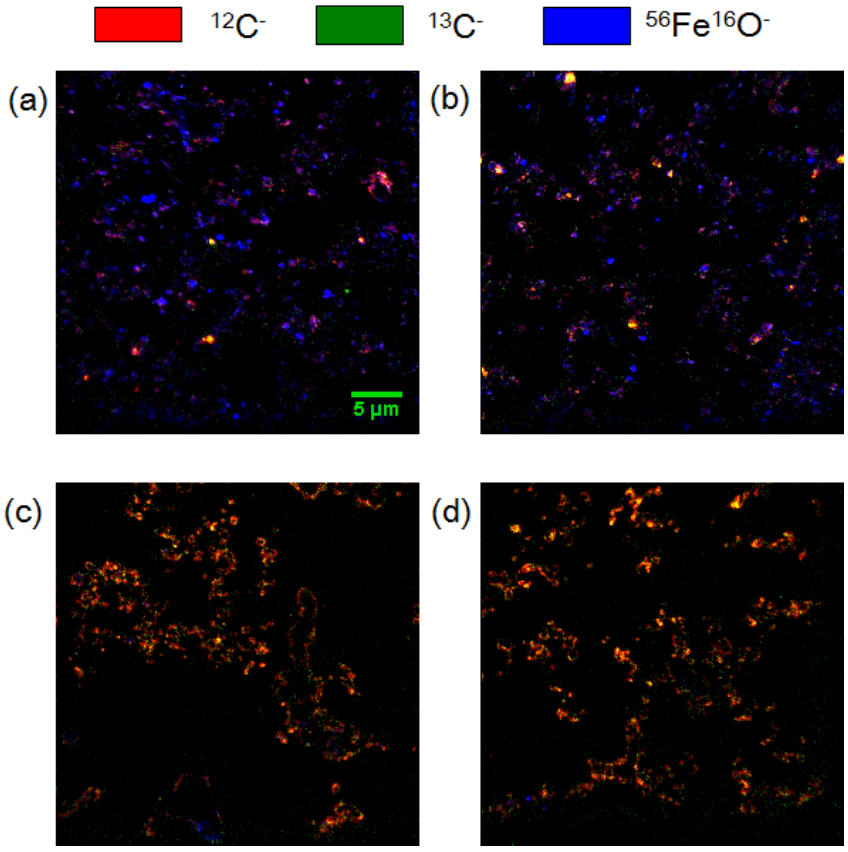

307

308 **Figure 4.** Representative NanoSIMS images of $^{12}C^-$, $^{13}C^-$, $^{56}Fe^{16}O^-$ from different anaerobic pre-
309 treatments (35 × 35 µm with a 256 × 256 pixel resolution). (a) Control: continuous aerobic phase
310 during the pre-treatment; (b) 4-day anaerobic pre-treatment: 8-day aerobic phase followed by 4-
311 day anaerobic phase during the pre-treatment; (c) 8-day anaerobic pre-treatment: 4-day aerobic
312 phase followed by 8-day anaerobic phase during the pre-treatment; (d) 12-day anaerobic pre-
313 treatment: 12-day anaerobic phase during the pre-treatment. The mixture of red and blue yields
314 magenta. The mixture of red and green yields yellow, which indicates lignin-derived C.

315

316 **DISCUSSION**

A modern paradigm of soil organic matter posits that lignin-derived C is a relatively minor contributor to soil organic matter,[6] due in part to its low microbial C-use efficiency.[8,9] However, methodological challenges may have obscured the contributions of lignin-derived C to MAOM.[24,25] Although low C-use efficiency of lignin would decrease the retention of lignin-derived C in microbial biomass and necromass, lignin degradation products could also potentially sorb to soil minerals. Consistent with these ideas, we found that increasing the duration of a single anaerobic event from 0 to 12 days had dual and long-lasting impacts on the decomposition of lignin and significantly impacted its association with Fe mineral phases after a subsequent 317-day aerobic incubation. On one hand, lignin was depolymerized to a greater extent following longer durations of anaerobic pre-treatments, as indicated by cumulative $^{13}CO_2$ production from lignin C_β (Figure 1f). The extent of lignin mineralization was inversely related to its solid-phase partitioning, supporting the concept that lignin can be readily decomposed in the absence of physicochemical protection.[6] On the other hand, longer durations of anaerobic pre-treatments also led to increased association of lignin-derived C with Fe (oxyhydr)oxides at the end of the experiment, as indicated by extractions of bulk soil and NanoSIMS analyses of high-density clay-sized fractions (Figures 3 and 4). These findings indicated that the fragmentation and decomposition of lignin stimulated after the initial redox fluctuation also increased the preferential association of lignin fragments with Fe minerals. Our results can thus reconcile the short-term stimulation of lignin decomposition in fluctuating redox environments[23] with the preservation of lignin-derived C by Fe oxides observed previously.[15,17,18,44] Although the turnover times of Fe-associated lignin-derived C remain unknown, these coupled mechanisms could potentially explain recent observations of preferential accumulation of lignin decomposition products relative to other organic C compounds in Fe-rich tropical forest soils.

[15,16] These studies included samples from the Oxisol, Andisol, Ultisol and Inceptisol soil orders with varying Fe content and mineral compositions.

Long-term Impacts of Short-term Anaerobiosis on Lignin Decomposition. Lignin decomposition was suppressed during the anaerobic pre-treatment, but rapidly recovered following the reintroduction of O_2. The immediate source of increased CO_2 during 12 to 22 days was probably DOC which progressively accumulated during anaerobiosis in parallel with Fe reduction (Figures S1 and S2). Added lignin was not a likely source of the accumulated DOC given that lignin depolymerization is suppressed in the absence of O_2.[45] The fact that treatment differences in lignin decomposition did not manifest until four months later is consistent with progressive degradation of lignin macromolecules (> 1000 daltons) over time. Following polymer cleavage, low-molecular weight lignin fragments can be mineralized to CO_2 at much greater rates than initial high-molecular weight lignin since many bacteria, in addition to lignin-degrading fungi, can assimilate or oxidize low-molecular weight lignin derivatives.[27,31] In addition, this time lag might be related to the depletion of easily assimilable substrates (e.g. cellulose and proteins) and changes in microbial community composition or abundance after the anaerobic pre-treatments. Coincidentally, fungal diversity peaked after four months in another study of litter decomposition,[46] the same period when we observed highest mineralization rates of added lignin. Along with changes in microbial composition, hydroxyl radical ($^{\cdot}OH$) production via the oxidation of Fe(II) by hydrogen peroxide (H_2O_2), known as the Fenton reaction, may also have contributed to variation in lignin depolymerization among treatments. This reaction can contribute to lignin decomposition because $^{\cdot}OH$ nonspecifically cleaves the relatively stable ether bonds of lignin.[4,47] Iron-rich soils undergoing redox fluctuations may promote Fenton chemistry given that Fe(II) is produced via microbial metabolism, and H_2O_2 can

363 be generated via numerous enzymatic reactions or by the abiotic oxidation of Fe(II) by O_2
364 ($Fe(II)+O_2+H^+ \rightarrow Fe(III) + HO^{\cdot}_2$; $Fe(II) + H^+ + HO^{\cdot}_2 \rightarrow H_2O_2 + Fe(III)$).[23,48] Relative to the
365 control, higher Fe(II) concentrations were generated in the longer anaerobic pre-treatments after
366 12 days of anaerobiosis and slowly declined concomitant with Fe(II) oxidation over the
367 subsequent weeks (Figures S1 and S2). However, added lignin residues were also susceptible to
368 sorption to mineral surfaces, and lignin-derived C in the high-density clay-sized fractions was
369 altered by the anaerobic pre-treatments. The difference in lignin-derived C in the clay-sized
370 fraction between the 4- and 12-day anaerobic pre-treatments (5.6 μg C g^{-1}) was very similar to
371 differences in lignin decomposition to CO_2 (5.3 μg C g^{-1}). Thus, alteration of lignin sorption by
372 the anaerobic pre-treatments most likely controlled lignin cleavage and mineralization of lignin
373 C_β.

374 **Preferential Association of Lignin-derived C with Fe Minerals.** Consistent with our first
375 hypothesis, our ^{13}C measurements directly showed that lignin-derived C can provide significant
376 and relatively rapid contributions to MAOM which were disproportionately greater than C from
377 bulk litter. Our findings challenge the MEMS hypothesis,[8,9] where biochemically labile
378 compounds that are efficiently incorporated into microbial biomass are thought to preferentially
379 accumulate in MAOM relative to more biochemically complex plant compounds.[49] We
380 acknowledge that microbial residues are clearly important contributors to MAOM.[50] However,
381 the lignin decomposition products observed in the dense fraction and its clay-sized subset were
382 unlikely to have substantially been derived from microbial biomass given the small extent of
383 cumulative lignin mineralization to CO_2 (5.7%) relative to the much larger proportion of lignin-
384 derived C in the high-density fractions (clay-sized high-density fraction + coarse high-density
385 fraction, 48.2%; Figure 2). Two arguments can be made to support this conclusion. First, using

386 the usual definition of microbial C-use efficiency,[51] and even assuming an unusually high value
387 of 50% for added lignin propyl sidechain C_β,[11,13] only 5.7% of added lignin C_β would have
388 accumulated in microbial biomass. Second, stoichiometric calculations have shown that even for
389 the readily utilized substrate glucose, the ratio of biomass produced to glucose mass respired for
390 energy cannot exceed approximately 7:3.[52] Thus, assuming that the 5.7% mineralization of added
391 lignin C_β reflects its use for energy production, no more than 13 – 14% of the added C could
392 have accumulated in microbial biomass, even under ideal conditions. In fact, the proportion of
393 lignin C_β in biomass would have to be considerably smaller, because the most efficient
394 mechanism for microbial cleavage of lignin's abundant arylglycerol-β-aryl ether structure
395 releases C_β as the aldehyde moiety of glycolaldehyde,[53] which is a more oxidized C source than
396 glucose is. Our direct evidence of disproportionate lignin-derived C inputs to MAOM relative to
397 bulk litter-derived C bolsters other recent work suggesting that plant-derived compounds can
398 substantially contribute to MAOM.[54–56]

399 The results from dithionite and subsequent pyrophosphate extractions and NanoSIMS
400 images indicated that the accumulation of lignin-derived C in MAOM can be due in part to its
401 preferential association with Fe minerals relative to the litter-derived C, which supported our
402 second hypothesis. Compared with the litter-derived C, the increased lignin-derived C in
403 dithionite extractions of soil from the longer anaerobic pre-treatments, together with the evidence
404 of increased lignin degradation but no changes in reactive Fe phases, demonstrated preferential
405 sorption of lignin-derived C to Fe oxides.[15,17] We observed even greater lignin release in the
406 subsequent pyrophosphate extraction, echoing a previous finding that sequential extraction by
407 dithionite and pyrophosphate release distinct C pools.[37] The lignin-derived C extracted by
408 dithionite and pyrophosphate solutions likely contained low-molecular-weight decomposition

409 products (e.g. modified alkyl sidechain moieties with and without attached aromatics) given the
410 poor solubility of lignin macromolecules in water.[31] However, a much larger proportion of
411 remaining mineral-associated lignin-derived C resisted extraction in dithionite and
412 pyrophosphate, and was therefore likely to have remained in poorly soluble phenylpropanoid
413 polymers after the Fe phases were dissolved in the extractants.

414 The NanoSIMS data from the clay-sized dense fractions provided additional evidence
415 that this large pool of non-extractable lignin-derived C also showed a specific association with
416 Fe at the nanoscale relative to litter-derived C, and that these interactions were enhanced
417 following short-term anaerobiosis. Previous studies by NanoSIMS demonstrated that mineral
418 particles in the clay-sized fraction can act as nuclei for litter-derived organic C accumulation.[34,57]
419 Analogously, the SRO Fe phases regenerated following Fe reduction and Fe(II) oxidation in the
420 longer anaerobic pre-treatments (8- and 12-day; Figure S1) likely provided new mineral surfaces
421 to sorb lignin C. Lignin-derived C incorporation in MAOM was enhanced with increasing
422 durations of short-term anaerobiosis (from 0 to 12 days). Given that many ecosystems in addition
423 to Fe-rich tropical forests have been shown to experience short-term soil O_2 variability and
424 associated Fe reduction (e.g., Mediterranean grassland, drained peatland, Midwestern cropland,
425 montane meadow, urban lawn, temperate forest)[58–61] the redox-driven accrual of lignin-derived C
426 in MAOM could represent a generally important mechanism.

427 **Role of Molecular Composition in SOM Paradigms.** Our results show that lignin can represent
428 a significant source of MAOM and that its fate is sensitive to environmental factors which have
429 already been altered by climate change in this tropical forest, where an unusually severe drought
430 recently caused a large increase in soil O_2 availability.[62] A lack of O_2 is increasingly
431 acknowledged to influence the persistence of SOM via impacts on the bioenergetics of

decomposition and the consequent accumulation of reduced compounds,[63,55] but our results demonstrate that geochemical impacts of O_2 deprivation may be equally important. Our findings indicated that the fragmentation and decomposition of lignin stimulated after the initial redox fluctuation (and associated Fe redox cycling) also increased the association of lignin fragments with Fe minerals. Frequent O_2 fluctuations can potentially alter soil Fe composition by promoting Fe reduction and increasing or decreasing Fe crystallinity,[21,64] which could conceivably lead to net accrual or release of lignin-derived C. It thus remains uncertain how Fe-lignin associations might be affected by frequent O_2 fluctuations in the field, although aromatic C was showed to be selectively released during hematite reduction in a laboratory incubation.[65] Soils similar to those used in this experiment showed positive correlations among SRO Fe, a proxy for aromatic C content, and turnover rates of mineral-associated C.[36] More research is needed to evaluate the persistence of Fe-associated lignin in soils that experience O_2 fluctuations. To sum up, in a partial reconciliation between aspects of old and new paradigms of SOM, we show that lignin-derived C can indeed represent a disproportionate source of MAOM relative to bulk litter, in contrast to recent work which hypothesized a minor role for lignin-derived C in MAOM.[7–9] However, the persistence of lignin was not due to inherent recalcitrance: we also found that the contribution of lignin-derived C to MAOM varied crucially as a function of ecosystem context (i.e., redox-sensitive biogeochemical reactions), a key tenet of recent thinking about SOM.[6] Further resolving when, where, and how long different organic compounds can persist in soil along the decay continuum is key to improving our understanding of SOM persistence under global change.

ASSOCIATED CONTENT

Supporting Information.

Details about the sample preparation; data processing calculations; details about the selected chemical properties of soil samples; additional data on Fe reduction and DOC; additional data on NanoSIMS analysis; additional Mössbauer spectra and Mössbauer spectral fitting parameters.

AUTHOR INFORMATION

Corresponding Author

* Phone: (01) 515-294-7650; e-mail: stevenjh@iastate.edu.

Author Contributions

All authors contributed to research. The manuscript was primarily written by WH and SJH with contributions from KEH and AT. All authors have given approval to the final version of the manuscript.

Notes

The authors declare no competing financial interest.

ACKNOWLEDGMENTS

We thank Whendee Silver for insightful discussion on topics related to this paper and for facilitating access to the site. This work was supported in part by NSF grants DEB-1457805, DEB-1802745, and EAR-1331841 (the Luquillo Critical Zone Observatory). Production of synthetic lignins was partially funded by the DOE Great Lakes Bioenergy Research Center (DOE Office of Science BER DE-FC02-07ER64494) and by DOE Office of Science grant BER DE-SC0012742. The NanoSIMS analysis was supported by the National Natural Science Foundation of China (Grant No. 31670487).

REFERENCES

(1) Boerjan, W.; Ralph, J.; Baucher, M. Lignin Biosynthesis. *Annu. Rev. Plant Biol.* **2003**, *54* (1), 519–546. https://doi.org/10.1146/annurev.arplant.54.031902.134938.
(2) Melillo, J. M.; Aber, J. D.; Muratore, J. F. Nitrogen and Lignin Control of Hardwood Leaf Litter Decomposition Dynamics. *Ecology* **1982**, *63* (3), 621–626. https://doi.org/10.2307/1936780.
(3) Bollag, J.-M.; Dec, J.; Huang, P. M. Formation Mechanisms of Complex Organic Structures in Soil Habitats. In *Advances in Agronomy*; Sparks, D. L., Ed.; Academic Press, 1997; Vol. 63, pp 237–266. https://doi.org/10.1016/S0065-2113(08)60245-X.
(4) Hammel, K. E.; Kapich, A. N.; Jensen, K. A.; Ryan, Z. C. Reactive Oxygen Species as Agents of Wood Decay by Fungi. *Enzyme Microb. Technol.* **2002**, *30* (4), 445–453. https://doi.org/10.1016/S0141-0229(02)00011-X.
(5) Lehmann, J.; Kleber, M. The Contentious Nature of Soil Organic Matter. *Nature* **2015**, *528* (7580), 60–68. https://doi.org/10.1038/nature16069.
(6) Schmidt, M. W. I.; Torn, M. S.; Abiven, S.; Dittmar, T.; Guggenberger, G.; Janssens, I. A.; Kleber, M.; Kögel-Knabner, I.; Lehmann, J.; Manning, D. A. C.; et al. Persistence of Soil Organic Matter as an Ecosystem Property. *Nature* **2011**, *478* (7367), 49–56. https://doi.org/10.1038/nature10386.
(7) Grandy, A. S.; Neff, J. C. Molecular C Dynamics Downstream: The Biochemical Decomposition Sequence and Its Impact on Soil Organic Matter Structure and Function. *Sci. Total Environ.* **2008**, *404* (2–3), 297–307. https://doi.org/10.1016/j.scitotenv.2007.11.013.
(8) Cotrufo, M. F.; Wallenstein, M. D.; Boot, C. M.; Denef, K.; Paul, E. The Microbial Efficiency-Matrix Stabilization (MEMS) Framework Integrates Plant Litter Decomposition with Soil Organic Matter Stabilization: Do Labile Plant Inputs Form Stable Soil Organic Matter? *Glob. Change Biol.* **2013**, *19* (4), 988–995. https://doi.org/10.1111/gcb.12113.
(9) Cotrufo, M. F.; Soong, J. L.; Horton, A. J.; Campbell, E. E.; Haddix, M. L.; Wall, D. H.; Parton, W. J. Formation of Soil Organic Matter via Biochemical and Physical Pathways of Litter Mass Loss. *Nat. Geosci.* **2015**, *8* (10), 776–779. https://doi.org/10.1038/ngeo2520.
(10) Sokol, N. W.; Bradford, M. A. Microbial Formation of Stable Soil Carbon Is More Efficient from Belowground than Aboveground Input. *Nat. Geosci.* **2019**, *12* (1), 46. https://doi.org/10.1038/s41561-018-0258-6.
(11) Martin, J. P.; Haider, K.; Kassim, G. Biodegradation and Stabilization after 2 Years of Specific Crop, Lignin, and Polysaccharide Carbons in Soils. *Soil Sci. Soc. Am. J.* **1980**, *44* (6), 1250. https://doi.org/10.2136/sssaj1980.03615995004400060024x.
(12) Stott, D. E.; Kassim, G.; Jarrell, W. M.; Martin, J. P.; Haider, K. Stabilization and Incorporation into Biomass of Specific Plant Carbons during Biodegradation in Soil. *Plant Soil* **1983**, *70* (1), 15–26. https://doi.org/10.1007/BF02374746.
(13) Bahri, H.; Rasse, D. P.; Rumpel, C.; Dignac, M.-F.; Bardoux, G.; Mariotti, A. Lignin Degradation during a Laboratory Incubation Followed by 13C Isotope Analysis. *Soil Biol. Biochem.* **2008**, *40* (7), 1916–1922. https://doi.org/10.1016/j.soilbio.2008.04.002.
(14) Sokol, N. W.; Sanderman, J.; Bradford, M. A. Pathways of Mineral‐associated Soil Organic Matter Formation: Integrating the Role of Plant Carbon Source, Chemistry, and Point of Entry. *Glob. Change Biol.* **2019**, *25* (1), 12–24. https://doi.org/10.1111/gcb.14482.
(15) Coward, E. K.; Ohno, T.; Plante, A. F. Adsorption and Molecular Fractionation of Dissolved Organic Matter on Iron-Bearing Mineral Matrices of Varying Crystallinity. *Environ. Sci. Technol.* **2018**, *52* (3), 1036–1044. https://doi.org/10.1021/acs.est.7b04953.
(16) Kramer, M. G.; Sanderman, J.; Chadwick, O. A.; Chorover, J.; Vitousek, P. M. Long-Term Carbon Storage through Retention of Dissolved Aromatic Acids by Reactive Particles in Soil. *Glob. Change Biol.* **2012**, *18* (8), 2594–2605. https://doi.org/10.1111/j.1365-2486.2012.02681.x.
(17) Hall, S. J.; Silver, W. L.; Timokhin, V. I.; Hammel, K. E. Iron Addition to Soil Specifically Stabilized Lignin. *Soil Biol. Biochem.* **2016**, *98*, 95–98. https://doi.org/10.1016/j.soilbio.2016.04.010.
(18) Riedel, T.; Zak, D.; Biester, H.; Dittmar, T. Iron Traps Terrestrially Derived Dissolved Organic Matter at Redox Interfaces. *Proc. Natl. Acad. Sci.* **2013**, *110* (25), 10101–10105.

https://doi.org/10.1073/pnas.1221487110.
(19) Chorover, J.; Amistadi, M. K. Reaction of Forest Floor Organic Matter at Goethite, Birnessite and Smectite Surfaces. *Geochim. Cosmochim. Acta* **2001**, *65* (1), 95–109. https://doi.org/10.1016/S0016-7037(00)00511-1.
(20) Thompson, A.; Rancourt, D. G.; Chadwick, O. A.; Chorover, J. Iron Solid-Phase Differentiation along a Redox Gradient in Basaltic Soils. *Geochim. Cosmochim. Acta* **2011**, *75* (1), 119–133. https://doi.org/10.1016/j.gca.2010.10.005.
(21) Ginn, B.; Meile, C.; Wilmoth, J.; Tang, Y.; Thompson, A. Rapid Iron Reduction Rates Are Stimulated by High-Amplitude Redox Fluctuations in a Tropical Forest Soil. *Environ. Sci. Technol.* **2017**, *51* (6), 3250–3259. https://doi.org/10.1021/acs.est.6b05709.
(22) Winkler, P.; Kaiser, K.; Thompson, A.; Kalbitz, K.; Fiedler, S.; Jahn, R. Contrasting Evolution of Iron Phase Composition in Soils Exposed to Redox Fluctuations. *Geochim. Cosmochim. Acta* **2018**, *235*, 89–102. https://doi.org/10.1016/j.gca.2018.05.019.
(23) Hall, S. J.; Silver, W. L.; Timokhin, V. I.; Hammel, K. E. Lignin Decomposition Is Sustained under Fluctuating Redox Conditions in Humid Tropical Forest Soils. *Glob. Change Biol.* **2015**, *21* (7), 2818–2828. https://doi.org/10.1111/gcb.12908.
(24) Hernes, P. J.; Kaiser, K.; Dyda, R. Y.; Cerli, C. Molecular Trickery in Soil Organic Matter: Hidden Lignin. *Environ. Sci. Technol.* **2013**, *47* (16), 9077–9085. https://doi.org/10.1021/es401019n.
(25) Klotzbücher, T.; Kalbitz, K.; Cerli, C.; Hernes, P. J.; Kaiser, K. Gone or Just out of Sight? The Apparent Disappearance of Aromatic Litter Components in Soils. *SOIL* **2016**, *2* (3), 325–335. https://doi.org/10.5194/soil-2-325-2016.
(26) Eusterhues, K.; Rumpel, C.; Kleber, M.; Kögel-Knabner, I. Stabilisation of Soil Organic Matter by Interactions with Minerals as Revealed by Mineral Dissolution and Oxidative Degradation. *Org. Geochem.* **2003**, *34* (12), 1591–1600. https://doi.org/10.1016/j.orggeochem.2003.08.007.
(27) Haider, K.; Martin, J. P. Decomposition in Soil of Specifically 14C-Labeled Model and Cornstalk Lignins and Coniferyl Alcohol over Two Years as Influenced by Drying, Rewetting, and Additions of an Available C Substrate. *Soil Biol. Biochem.* **1981**, *13* (6), 447–450. https://doi.org/10.1016/0038-0717(81)90032-8.
(28) Dubinsky, E. A.; Silver, W. L.; Firestone, M. K. Tropical Forest Soil Microbial Communities Couple Iron and Carbon Biogeochemistry. *Ecology* **2010**, *91* (9), 2604–2612. https://doi.org/10.1890/09-1365.1.
(29) Barcellos, D.; O'Connell, C. S.; Silver, W.; Meile, C.; Thompson, A. Hot Spots and Hot Moments of Soil Moisture Explain Fluctuations in Iron and Carbon Cycling in a Humid Tropical Forest Soil. *Soil Syst.* **2018**, *2* (4), 59. https://doi.org/10.3390/soilsystems2040059.
(30) Bloomfield, J.; Vogt, K. A.; Vogt, D. J. Decay Rate and Substrate Quality of Fine Roots and Foliage of Two Tropical Tree Species in the Luquillo Experimental Forest, Puerto Rico. *Plant Soil* **1993**, *150* (2), 233–245. https://doi.org/10.1007/BF00013020.
(31) Kirk, T. K.; Farrell, R. L. Enzymatic "Combustion": The Microbial Degradation of Lignin. *Annu. Rev. Microbiol. USA* **1987**, *41*, 465–505. https://doi.org./10.1146/annurev.mi.41.100187.002341.
(32) Hall, S. J.; Huang, W.; Hammel, K. E. An Optical Method for Carbon Dioxide Isotopes and Mole Fractions in Small Gas Samples: Tracing Microbial Respiration from Soil, Litter, and Lignin. *Rapid Commun. Mass Spectrom.* **2017**, *31* (22), 1938–1946. https://doi.org/10.1002/rcm.7973.
(33) Huang, W.; Hall, S. J. Large Impacts of Small Methane Fluxes on Carbon Isotope Values of Soil Respiration. *Soil Biol. Biochem.* **2018**, *124*, 126–133. https://doi.org/10.1016/j.soilbio.2018.06.003.
(34) Vogel, C.; Mueller, C. W.; Höschen, C.; Buegger, F.; Heister, K.; Schulz, S.; Schloter, M.; Kögel-Knabner, I. Submicron Structures Provide Preferential Spots for Carbon and Nitrogen Sequestration in Soils. *Nat. Commun.* **2014**, *5*, 2947. https://doi.org/10.1038/ncomms3947.
(35) Kaiser, K.; Guggenberger, G. Distribution of Hydrous Aluminium and Iron over Density Fractions Depends on Organic Matter Load and Ultrasonic Dispersion. *Geoderma* **2007**, *140* (1), 140–146. https://doi.org/10.1016/j.geoderma.2007.03.018.
(36) Hall, S. J.; Berhe, A. A.; Thompson, A. Order from Disorder: Do Soil Organic Matter Composition and Turnover Co-Vary with Iron Phase Crystallinity? *Biogeochemistry* **2018**, *140* (1), 93–110.

https://doi.org/10.1007/s10533-018-0476-4.
(37) Coward, E. K.; Thompson, A. T.; Plante, A. F. Iron-Mediated Mineralogical Control of Organic Matter Accumulation in Tropical Soils. *Geoderma* **2017**, *306*, 206–216. https://doi.org/10.1016/j.geoderma.2017.07.026.
(38) Wagai, R.; Mayer, L. M.; Kitayama, K.; Shirato, Y. Association of Organic Matter with Iron and Aluminum across a Range of Soils Determined via Selective Dissolution Techniques Coupled with Dissolved Nitrogen Analysis. *Biogeochemistry* **2013**, *112* (1), 95–109. https://doi.org/10.1007/s10533-011-9652-5.
(39) Chen, C.; Thompson, A. Ferrous Iron Oxidation under Varying PO_2 Levels: The Effect of Fe(III)/Al(III) Oxide Minerals and Organic Matter. *Environ. Sci. Technol.* **2018**, *52* (2), 597–606. https://doi.org/10.1021/acs.est.7b05102.
(40) Schindelin, J.; Arganda-Carreras, I.; Frise, E.; Kaynig, V.; Longair, M.; Pietzsch, T.; Preibisch, S.; Rueden, C.; Saalfeld, S.; Schmid, B.; et al. Fiji: An Open-Source Platform for Biological-Image Analysis. *Nat. Methods* **2012**, *9*, 676–682.
(41) Otsu, N. A Threshold Selection Method from Gray-Level Histograms. *IEEE Trans. Syst. Man Cybern.* **1979**, *9* (1), 62–66. https://doi.org/10.1109/TSMC.1979.4310076.
(42) Bates, D.; Mächler, M.; Bolker, B.; Walker, S. Fitting Linear Mixed-Effects Models Using Lme4. *J. Stat. Softw.* **2015**, *67* (1), 1–48.
(43) R Core Team. *R: A Language and Environment for Statistical Computing*; R Foundation for Statistical Computing, Vienna, Austria: Vienna, Austria, 2018.
(44) Shields, M. R.; Bianchi, T. S.; Gélinas, Y.; Allison, M. A.; Twilley, R. R. Enhanced Terrestrial Carbon Preservation Promoted by Reactive Iron in Deltaic Sediments. *Geophys. Res. Lett.* **2016**, *43* (3), 1149–1157. https://doi.org/10.1002/2015GL067388.
(45) Benner, R.; Maccubbin, A. E.; Hodson, R. E. Anaerobic Biodegradation of the Lignin and Polysaccharide Components of Lignocellulose and Synthetic Lignin by Sediment Microflora. *Appl. Environ. Microbiol.* **1984**, *47* (5), 998–1004.
(46) Voříšková, J.; Baldrian, P. Fungal Community on Decomposing Leaf Litter Undergoes Rapid Successional Changes. *ISME J.* **2013**, *7* (3), 477–486. https://doi.org/10.1038/ismej.2012.116.
(47) Wood, P. Pathways for Production of Fenton's Reagent by Wood-Rotting Fungi. *FEMS Microbiol. Rev.* **1994**, *13* (2–3), 313–320.
(48) Hall, S. J.; Silver, W. L. Iron Oxidation Stimulates Organic Matter Decomposition in Humid Tropical Forest Soils. *Glob. Change Biol.* **2013**, *19* (9), 2804–2813. https://doi.org/10.1111/gcb.12229.
(49) Cyle, K. T.; Hill, N.; Young, K.; Jenkins, T.; Hancock, D.; Schroeder, P. A.; Thompson, A. Substrate Quality Influences Organic Matter Accumulation in the Soil Silt and Clay Fraction. *Soil Biol. Biochem.* **2016**, *103*, 138–148. https://doi.org/10.1016/j.soilbio.2016.08.014.
(50) Kallenbach, C. M.; Frey, S. D.; Grandy, A. S. Direct Evidence for Microbial-Derived Soil Organic Matter Formation and Its Ecophysiological Controls. *Nat. Commun.* **2016**, *7*, 13630. https://doi.org/10.1038/ncomms13630.
(51) Manzoni, S.; Taylor, P.; Richter, A.; Porporato, A.; Ågren, G. I. Environmental and Stoichiometric Controls on Microbial Carbon-Use Efficiency in Soils. *New Phytol.* **2012**, *196* (1), 79–91. https://doi.org/10.1111/j.1469-8137.2012.04225.x.
(52) Watve, M.; Shejval, V.; Sonawane, C.; Rahalkar, M.; Matapurkar, A.; Shouche, Y.; Patole, M.; Phadnis, N.; Champhenkar, A.; Damle, K.; et al. The "K" Selected Oligophilic Bacteria: A Key to Uncultured Diversity? *Curr. Sci.* **2000**, *78* (12), 1535–1542.
(53) Hammel, K. E.; Mozuch, M. D.; Jensen, K. A.; Kersten, P. J. H_2O_2 Recycling during Oxidation of the Arylglycerol-β-Aryl Ether Lignin Structure by Lignin Peroxidase and Glyoxal Oxidase. *Biochemistry* **1994**, *33* (45), 13349–13354. https://doi.org/10.1021/bi00249a022.
(54) Córdova, S. C.; Olk, D. C.; Dietzel, R. N.; Mueller, K. E.; Archontouilis, S. V.; Castellano, M. J. Plant Litter Quality Affects the Accumulation Rate, Composition, and Stability of Mineral-Associated Soil Organic Matter. *Soil Biol. Biochem.* **2018**, *125*, 115–124. https://doi.org/10.1016/j.soilbio.2018.07.010.

(55) Angst, G.; Mueller, K. E.; Kögel-Knabner, I.; Freeman, K. H.; Mueller, C. W. Aggregation Controls the Stability of Lignin and Lipids in Clay-Sized Particulate and Mineral Associated Organic Matter. *Biogeochemistry* **2017**, *132* (3), 307–324. https://doi.org/10.1007/s10533-017-0304-2.

(56) Rumpel, C.; Baumann, K.; Remusat, L.; Dignac, M.-F.; Barré, P.; Deldicque, D.; Glasser, G.; Lieberwirth, I.; Chabbi, A. Nanoscale Evidence of Contrasted Processes for Root-Derived Organic Matter Stabilization by Mineral Interactions Depending on Soil Depth. *Soil Biol. Biochem.* **2015**, *85*, 82–88. https://doi.org/10.1016/j.soilbio.2015.02.017.

(57) Yu, G.; Xiao, J.; Hu, S.; Polizzotto, M. L.; Zhao, F.; McGrath, S. P.; Li, H.; Ran, W.; Shen, Q. Mineral Availability as a Key Regulator of Soil Carbon Storage. *Environ. Sci. Technol.* **2017**, *51* (9), 4960–4969. https://doi.org/10.1021/acs.est.7b00305.

(58) Yang, W. H.; Liptzin, D. High Potential for Iron Reduction in Upland Soils. *Ecology* **2015**, *96* (7), 2015–2020. https://doi.org/10.1890/14-2097.1.

(59) Hall, S. J.; Weintraub, S. R.; Bowling, D. R. Scale-Dependent Linkages between Nitrate Isotopes and Denitrification in Surface Soils: Implications for Isotope Measurements and Models. *Oecologia* **2016**, *181* (4), 1221–1231. https://doi.org/10.1007/s00442-016-3626-1.

(60) Krichels, A.; DeLucia, E. H.; Sanford, R.; Chee-Sanford, J.; Yang, W. H. Historical Soil Drainage Mediates the Response of Soil Greenhouse Gas Emissions to Intense Precipitation Events. *Biogeochemistry* **2019**, *142* (3), 425–442. https://doi.org/10.1007/s10533-019-00544-x.

(61) Fimmen, R. L.; Richter, D. deB.; Vasudevan, D.; Williams, M. A.; West, L. T. Rhizogenic Fe–C Redox Cycling: A Hypothetical Biogeochemical Mechanism That Drives Crustal Weathering in Upland Soils. *Biogeochemistry* **2008**, *87* (2), 127–141. https://doi.org/10.1007/s10533-007-9172-5.

(62) O'Connell, C. S.; Ruan, L.; Silver, W. L. Drought Drives Rapid Shifts in Tropical Rainforest Soil Biogeochemistry and Greenhouse Gas Emissions. *Nat. Commun.* **2018**, *9* (1), 1348. https://doi.org/10.1038/s41467-018-03352-3.

(63) Keiluweit, M.; Wanzek, T.; Kleber, M.; Nico, P.; Fendorf, S. Anaerobic Microsites Have an Unaccounted Role in Soil Carbon Stabilization. *Nat. Commun.* **2017**, *8* (1), 1771. https://doi.org/10.1038/s41467-017-01406-6.

(64) Thompson, A.; Chadwick, O. A.; Boman, S.; Chorover, J. Colloid Mobilization during Soil Iron Redox Oscillations. *Environ. Sci. Technol.* **2006**, *40* (18), 5743–5749. https://doi.org/10.1021/es061203b.

(65) Adhikari, D.; Yang, Y. Selective Stabilization of Aliphatic Organic Carbon by Iron Oxide. *Sci. Rep.* **2015**, *5* (1), 11214. https://doi.org/10.1038/srep11214.